Proc. Natl. Acad. Sci. USA
Vol. 88, pp. 8174–8178, September 1991
Biochemistry

Assembly of the *Escherichia coli* 30S ribosomal subunit reveals protein-dependent folding of the 16S rRNA domains

VALSAN MANDIYAN*, SANTA J. TUMMINIA*, JOSEPH S. WALL†, JAMES F. HAINFELD†, AND MILOSLAV BOUBLIK*‡

*Roche Institute of Molecular Biology, Roche Research Center, Nutley, NJ 07110; and †Department of Biology, Brookhaven National Laboratory, Upton, NY 11973

Communicated by Masayasu Nomura, June 13, 1991 (received for review April 14, 1991)

ABSTRACT **Protein–nucleic acid interactions involved in the assembly process of the *Escherichia coli* 30S ribosomal subunit were quantitatively analyzed by high-resolution scanning transmission electron microscopy. The *in vitro* reconstituted ribonucleoprotein (core) particles were characterized by their morphology, mass, and radii of gyration. During the assembly of the 30S subunit, the 16S rRNA underwent significant conformational changes that were governed by the cooperative interactions of the ribosomal proteins. The sequential association of the first 12 proteins with the 16S rRNA resulted in the formation of core particles containing up to three mass centers at distinct stages of the assembly process. These globular mass centers may correspond to the three major domains (5′, central, and 3′) of the 16S rRNA. Through the subsequent interactions of the late assembly proteins with the 16S rRNA, two of the three domains merge, yielding the basic structural traits of the native 30S subunit. The fine morphological features of the native 30S subunit became distinctly resolved only after the addition of the full complement of proteins. The fully reconstituted 30S subunits are active in polyphenylalanine synthesis assays. Visualization of the assembly mechanism of the *E. coli* 30S ribosomal subunit revealed domain-specific folding of the 16S rRNA through the formation of distinct intermediate core particles hitherto not observed.**

Ribosomes are ubiquitous macromolecular assemblies of proteins and ribonucleic acids involved in protein biosynthesis. This bipartite cellular organelle is composed of a large and a small subunit. The structure–function relationship of the small (30S) ribosomal subunit of *Escherichia coli* has been extensively studied. This subunit is actively involved in the initiation of protein synthesis by its interactions with initiation factors, messenger RNAs, transfer RNAs, and the large (50S) ribosomal subunit (1–4). The 30S subunit possesses characteristic structural features known as the head, body, cleft, and platform (5, 6) and is composed of a single 16S rRNA molecule and 21 different ribosomal proteins (S1–S21). Several ribosomal proteins interact with the 16S rRNA through a sequential and cooperative process as revealed from the *in vitro* assembly of the 30S subunit (7–9). Results obtained from these studies led to the classification of the proteins as primary binding proteins, which bind directly to the 16S rRNA, and secondary binding proteins, which require the previous association of the primary binding proteins. Apart from being the structural base for protein interactions, the 16S rRNA has an established role in protein biosynthesis (10–14). However, the role of the ribosomal proteins in ribosome structure and function remains unclear.

Scanning transmission electron microscopy (STEM) was used to quantitatively evaluate the conformational changes induced in the 16S rRNA molecule by its interactions with the ribosomal proteins under nondenaturing conditions (15). Unlike other physical techniques that yield statistically averaged values, STEM provides the physical characteristics of individual macromolecules. Along with high-resolution morphology, quantitative parameters such as mass (kDa), mass per unit length, and radius of gyration (R_G), were the major criteria used in the evaluation of the rRNA–protein interactions.

MATERIALS AND METHODS

Isolation of Ribosomes and Their Components. Ribosomes and ribosomal subunits were prepared from frozen *E. coli* MRE 600 cells as described (16, 17).

Proteins from the 30S subunit were extracted twice with $Mg(OAc)_2$/acetic acid, dialyzed against 6% acetic acid, and lyophilized. The mixture of 21S proteins was initially separated on a phosphocellulose column (18). The eluted proteins were dialyzed against 6% acetic acid, lyophilized, and further purified by HPLC on an Altex RPSC C3 semipreparative column (19). The proteins were identified as described (16).

The 16S rRNA was prepared from 30S subunits by the phenol/chloroform extraction method and its purity and integrity were checked by agarose gel electrophoresis (16).

Complexes of 16S rRNA with Ribosomal Proteins. Sequential addition of the ribosomal proteins to the 16S rRNA was carried out according to the assembly map of Held *et al.* (figure 1 in ref. 7) except in the case of S13. Protein S13 was added after the association of S7 and S19 because of its ability to crosslink with both of these proteins (20). The ribosomal proteins and the 16S rRNA used in the reconstitutions were incubated separately at 40°C for 10 min. 16S rRNA was reconstituted with a 3-fold molar excess of ribosomal proteins and incubated in a stepwise manner from 40°C to 50°C over 90 min. These conditions yield the highest number of reconstituted particles (as judged by STEM imaging) and were found to be optimal for the reconstitution of both natural as well as synthetic 16S rRNA (21). The final ionic conditions of the reconstitution mixture were 30 mM Hepes·KOH, pH 7.5/333 mM KCl/20 mM $Mg(OAc)_2$. The reconstituted RNA–protein complexes were separated on 15–30% sucrose gradients [20 mM Hepes·KOH, pH 7.5/100 mM KCl/15 mM $Mg(OAc)_2$/10 mM 2-mercaptoethanol] at 93,000 × *g* for 19 hr in an SW28 rotor. The peak fractions were dialyzed exhaustively against 10 mM Hepes·KOH, pH 7.5/60 mM KCl/2 mM $Mg(OAc)_2$/10 mM 2-mercaptoethanol (buffer I). In addition to the ribosomal particles being stable under these ionic conditions, buffer I has the advantage of low background noise for high-resolution STEM imaging. The 16S rRNA–protein complexes recovered from the sucrose gradients were pelleted at 200,000 × *g* for 16 hr and assayed for protein content by 18% SDS/PAGE (16).

The publication costs of this article were defrayed in part by page charge payment. This article must therefore be hereby marked "*advertisement*" in accordance with 18 U.S.C. §1734 solely to indicate this fact.

Abbreviations: STEM, scanning transmission electron microscopy; R_G, radius of gyration; EF, elongation factor.

‡To whom reprint requests should be addressed.

Biological Activity. The reconstituted complexes were assayed for their ability to carry out poly(U)-dependent polyphenylalanine synthesis (17). Complexes and native 30S and 50S subunits were independently activated by incubation at 40°C for 30 min. The reconstituted complexes were mixed with native 50S subunits in a 1:1.6 molar ratio. The final concentration of activated particles was 20 nM and the final assay conditions were as follows: 50 mM Hepes·KOH, pH 7.5/50 mM NH_4Cl/20 mM $Mg(OAc)_2$/5 mM phospho*enol*pyruvate/2 mM ATP/5 mM 2-mercaptoethanol/pyruvate kinase (0.76 mg/ml)/1 mM GTP/elongation factor (EF)-Tu (67.2 pmol/ml)/EF-G (0.014 mg/ml)/poly(U) (20 μg/ml). [^{3}H]Phenylalanine tRNA was added to each sample to a final concentration of 300 pmol/ml, and the samples were incubated at 37°C for 30 min. The reactions were stopped by trichloroacetic acid precipitation, and reaction products were filtered through nitrocellulose membranes, washed with 5% trichloroacetic acid, dissolved in scintillation fluid, and assayed.

Electron Microscopy. High-resolution electron microscopic imaging, mass measurements, and calculations of R_G were carried out with Brookhaven STEM as described (15). Several hundred particles were measured in each set of experiments.

RESULTS AND DISCUSSION

The assembly of the *E. coli* 30S ribosomal subunit involves the sequential association of 21 different proteins to a single 16S rRNA molecule as shown in Fig. 1 (7). High-resolution imaging of the effects of the association of the six primary binding proteins (S4, S8, S15, S20, S17, and S7) on 16S rRNA structure provided direct evidence for conformational changes in 16S rRNA during the initial stages of the assembly process (16). These proteins transformed the loosely coiled 16S rRNA molecule into a "medusa-like" structure characterized by an electron-dense region corresponding to the first observed mass center of the 16S rRNA and a "tail" consisting of loosely attached filaments (16).

Reconstitution of the 16S rRNA with the primary binding proteins and the first of the secondary binding proteins, S19, increased the mass of the core particles to 642 ± 23 kDa in agreement with the theoretical data (Table 1, Complex I) but did not significantly change their morphology (Fig. 2*a*). The decrease in the R_G value (95 ± 10 Å) implies partial condensation of the 16S rRNA.

The subsequent binding of S13 (Table 1, Complex II) increased the mass of the core particles to 651 ± 29 kDa and the R_G value to 100 ± 8 Å. The presence of S7–S13–S19

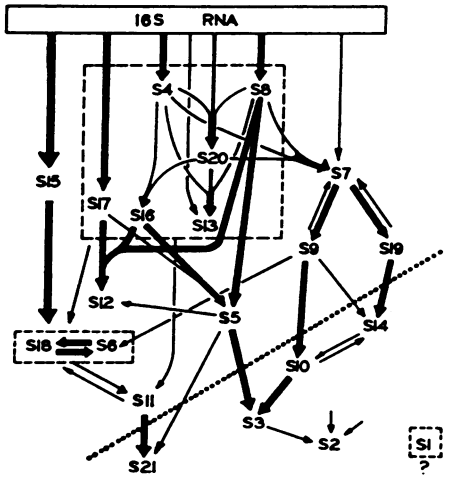

FIG. 1. Assembly map of the *E. coli* 30S subunits *in vitro*. (Reprinted from ref. 7 with permission. Copyright 1974 American Society of Biological Chemists.)

crosslinks in 30S subunits (20), as well as the distance (≈52 Å) between the centers of these proteins (22, 23), may attribute this effect on the R_G value to the formation of the nucleus of the second mass center (Fig. 2*b*). Multiple binding sites for S13 on the 16S rRNA molecule have been reported (24, 25), suggesting that S13 might be loosely bound between different locations. However, neutron scattering (22) and chemical protection studies (26) clearly associate protein S13 with the 3′ major domain of the 16S rRNA.

The subsequent addition of S9 (Table 1, Complex III) led to the formation of core particles with two well-developed electron-dense mass centers as well as rudiments of a third center (Fig. 2*c*). The association of S9 along with S7 and S19 stabilizes the 3′ major domain of the 16S rRNA for protein binding (27). It has been shown that S9 crosslinks to two regions in the 3′ domain, one at nucleotide 954 and the other in the nucleotide 1130 region (24). Chemical protection studies support the interaction in the nucleotide 1125 region, but protection is also observed in the nucleotide 1280 region (27). The presence of S9 in the core complex may bring the nucleotide 1130 helical region closer to the S7 and S19 binding sites (nucleotide 1280 region). This assumption is supported by UV irradiation-induced RNA–RNA crosslinks between nucleotides 1125–1127 and 1280–1281 (24). The established existence of protein–protein contacts between S7, S9, and S19 (20) and the proximity of S7 and S9 (22) suggest that the observed second mass center is probably due to the folding of the rRNA stabilized by protein–protein contacts. Evidence for the formation of two mass centers (independent nucleation sites) (28) also arises from reconstitution studies where the 16S rRNA folded into a two-domain structure, one controlled by S4 at the 5′ domain and the other controlled by S7 at the 3′ domain (28, 29).

The association of S18 (Table 1, Complex IV) enhanced the contours of the two domains (Fig. 2*d*). Although crosslinking data (24) show that S18 interacts with nucleotide C846, there are considerable discrepancies as to the binding properties of S18. According to Held *et al.* (7), the binding of S18 depends on the simultaneous presence of S6, the next protein in the assembly sequence. However, Gregory *et al.* (30) reported that S18 can be bound to the 16S rRNA in the presence of S8 and S15 alone. Analysis of the gel patterns of these RNA–protein complexes (Fig. 3, lane 4) indicates a considerable amount of S18 binding to 16S rRNA, which is enhanced by subsequent interaction with S6.

The decrease in R_G from 98 to 92 Å after the binding of S6 (Table 1, Complex V) indicates substantial rearrangement of the core structure as is evident from the formation of a third distinct mass center (Fig. 2*e*), which is connected to the previously formed centers by fine filamentous structures. These structural changes observed after the interaction of S6 appear to be in disagreement with the results reported by Nomura *et al.* (31) in which the omission of S6 yielded particles with the same S value as native 30S subunits. However, it is possible that S6, like S16 or S18, plays an important role in the assembly process, which may be masked because the presence of all of the other proteins results in cooperative interactions leading to the formation of particles apparently similar to the native subunits (32). Secondary structure models have delineated the 16S rRNA into three major domains (5′, central, and 3′) held together by a pseudoknot structure, which forms a "topographical center" (24, 33–35). The mass centers observed at this stage of the assembly process are analogous to the three major domains of the 16S rRNA, which are held together by the topographical center. In addition to proteins S6 and S18 [only 33 Å apart (22)], the core particles contain S8 and S15, which are known to stabilize the central domain of the 16S rRNA (30, 36). S15 binding enhances the chemical reactivity of several bases in the central domain of 16S rRNA, providing crucial contact

Table 1. Molecular mass and R_G of *E. coli* 16S rRNA and 16S rRNA associated with up to 21 ribosomal (S) proteins in buffer I

Complex		Mass,* kDa	Mass ± SD, kDa	R_G ± SD, Å
	16S rRNA	550	551 ± 22	114 ± 20
i	16S rRNA + S4	573	574 ± 25	102 ± 13
ii	16S rRNA + S4, S8	587	586 ± 21	97 ± 14
iii	16S rRNA + S4, S8, S15	597	592 ± 26	91 ± 14
iv	16S rRNA + S4, S8, S15, S20	606	615 ± 24	94 ± 13
v	16S rRNA + S4, S8, S15, S20, S17	615	621 ± 24	94 ± 12
vi	16S rRNA + S4, S8, S15, S20, S17, S7	635	625 ± 25	108 ± 11
I	16S rRNA + S4, S8, S15, S20, S16/17, S7, S19	654	642 ± 23	95 ± 10
II	16S rRNA + S4, S8, S15, S20, S16/17, S7, S19, S13	667	651 ± 29	100 ± 8
III	16S rRNA + S4, S8, S15, S20, S16/17, S7, S19, S13, S9	682	659 ± 26	99 ± 8
IV	16S rRNA + S4, S8, S15, S20, S16/17, S7, S19, S13, S9, S18	691	665 ± 36	98 ± 10
V	16S rRNA + S4, S8, S15, S20, S16/17, S7, S19, S13, S9, S18, S6	707	683 ± 37	92 ± 12
VI	16S rRNA + S4, S8, S15, S20, S16/17, S7, S19, S13, S9, S18, S6, S11	721	695 ± 40	91 ± 11
VII	16S rRNA + S4, S8, S15, S20, S16/17, S7, S19, S13, S9, S18, S6, S11, S5	738	701 ± 39	95 ± 12
VIII	16S rRNA + S4, S8, S15, S20, S16/17, S7, S19, S13, S9, S18, S6, S11, S5, S12	752	710 ± 43	92 ± 11
IX	16S rRNA + S4, S8, S15, S20, S16/17, S7, S19, S13, S9, S18, S6, S11, S5, S12, S14	763	718 ± 35	84 ± 8
X	16S rRNA + S4, S8, S15, S20, S16/17, S7, S19, S13, S9, S18, S6, S11, S5, S12, S14, S10	755	738 ± 36	83 ± 7
XI	16S rRNA + S4, S8, S15, S20, S16/17, S7, S19, S13, S9, S18, S6, S11, S5, S12, S14, S10, S3	801	773 ± 27	77 ± 7
XII	16S rRNA + S4, S8, S15, S20, S16/17, S7, S19, S13, S9, S18, S6, S11, S5, S12, S14, S10, S3, S2	827	805 ± 24	73 ± 6
XIII	16S rRNA + S4, S8, S15, S20, S16/17, S7, S19, S13, S9, S18, S6, S11, S5, S12, S14, S10, S3, S2, S21	836	819 ± 32	75 ± 5
XIV	16S rRNA + TP30	900	814 ± 61	73 ± 6
	30S *E. coli*	900	872 ± 41	70 ± 4

Data for Complexes i–vi are from our previous results (16).
*Theoretical values, assuming stoichiometric binding of the proteins.

sites for the binding of S6 and S18. Chemical protection studies indicate that S6 and S18 protect the 695 and 800 regions (37) and intra-16S rRNA crosslinking *in vivo* (24) implies the close proximity of these two regions. Thus, S18 and S6 binding might have brought these two regions of the 16S rRNA together, resulting in the formation of a third mass center. Since the total mass (≈700 kDa) is distributed almost equally between the three mass centers—i.e., each center is ≈250 ± 50 kDa—the major mass contribution in these three domains stems from the 16S rRNA.

The sequential binding of S11 to 16S rRNA (Table 1, Complex VI) induced striking changes in the appearance of the core particles (Fig. 2*f*), which exhibited an increase in mass but no significant difference in R_G. Association of S11 with the 16S rRNA led to the partial merging of the three mass centers with a negligible effect on the center of gravity. This shift obscured the fine filamentous structures previously observed between these mass centers. It has been shown that S11 crosslinks to the 690 stem–loop region of the central domain (24), and protein–protein crosslinks revealed that S11 is in the vicinity of S18 (20). It is interesting that a protein with a precise binding site in the central domain could induce such a dramatic effect in the assembly process. The merging of the three mass centers caused by the interaction of S11 may be the result of conformational rearrangements of the 16S rRNA in the core particles as is reflected in the chemical protection of a large region of the 16S rRNA (36).

The trend of significant morphological changes in the core particles continued after the binding of S5 and S12 (Table 1, Complexes VII and VIII; Fig. 4 *a* and *b*, respectively). These core complexes possess a body (405 ± 25 kDa and 410 ± 30 kDa) and a loosely attached head (299 ± 11 kDa and 307 ± 17 kDa). It has been shown that the body is formed from the central and 5′ domains, while the head is formed from the 3′ major domain of the 16S rRNA (22, 24, 38–42). The head observed at this stage of assembly favors the independent formation of the 3′ domain (27). Binding of S5 and S12 mediates merging of the central domain with the 5′ domain. This conclusion is supported by S4–S5 and S5–S8 crosslinks as well as the S4–S5–S8 triple crosslink previously observed in the native 30S subunits (20). Since S4 and S8 are assembly initiator proteins of the 5′ and central domains (7), S5 may act as a bridging protein between these two domains. From our studies, it is evident that S5 alone is not sufficient to cause the complete merging of the domains and requires the supportive interaction of S12, which has adjacent binding sites on the

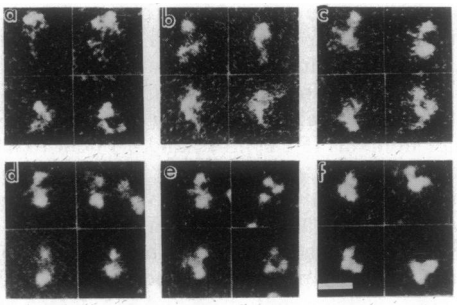

FIG. 2. STEM images of *E. coli* reconstituted core particles from complex I (*a*), complex II (*b*), complex III (*c*), complex IV (*d*), complex V (*e*), complex VI (*f*). (Bar = 300 Å.)

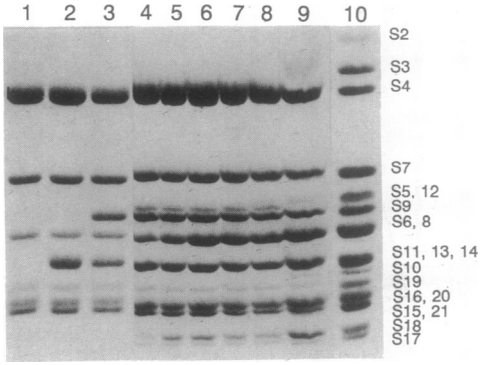

FIG. 3. The protein content of isolated core particles was analyzed by SDS/18% PAGE. Lanes 1–8, complexes I–VIII, respectively; lane 9, complex XIV. The same concentration (1.5 A_{260} units) of native 30S subunits was used as a reference (lane 10). Complexes IX–XIII were analyzed similarly (data not shown).

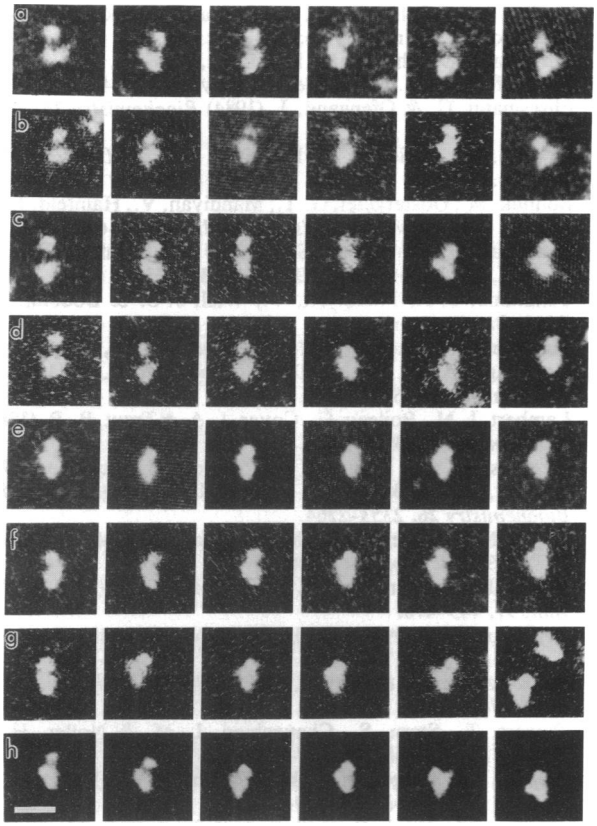

FIG. 4. STEM images of *E. coli* reconstituted core particles from complex VII (*a*), complex VIII (*b*), complex IX (*c*), complex X (*d*), complex XI (*e*), complex XII (*f*), complex XIII (*g*), complex XIV (*h*). (Bar = 300 Å.)

16S rRNA (36). Further studies provided evidence that S5 association stimulates the binding of S12 (7, 36, 40). Single protein omission experiments established that the lack of S5 has a significant effect on the sedimentation coefficient of core particles (43), which may be due to the absence of merging of the central and 5′ domains. Interestingly, S5 and S12 are part of the domain where EF-Tu and EF-G interact with the 30S subunit (44, 45). Since S5 and S12 are involved in conferring translational fidelity in protein biosynthesis (46), it appears that this effect depends on the integration of the 5′ and central domains of the 16S rRNA.

Association of proteins S14 and S10 (Table 1, Complexes IX and X), both of which were mapped to the head of native 30S subunits (41) within a distance of 36 Å (20, 22), led to the enhancement of this characteristic feature (Fig. 4 *c* and *d*), but not to its integration with the body as in the native 30S subunits. Studies have shown that the binding of S10 is dependent on the presence of S9 and that both S14 and S10 stimulate mutual assembly (7, 8). Although S14 and S10 along with S7, S9, and S19 protect almost the entire 3′ domain from nuclease digestion (47), chemical modifications reveal only limited protection in the 16S rRNA (26), suggesting that the assembly of S14 and S10 involves mostly protein–protein interactions.

The interaction of protein S3 followed by S2 (Table 1, Complexes XI and XII) led to the merging of the head and body (Fig. 4 *e* and *f*), and the formation of a particle (805 ± 24 kDa) that resembled the native 30S subunits (Fig. 5*j*). Crosslinking (20) and chemical modification studies (26) indicate that S3 is in the vicinity of S2. The complete suppression of the partition between the head and body is in agreement with immunoelectron microscopic localization of S3 and S2 (41). A comparison of the results of sequential

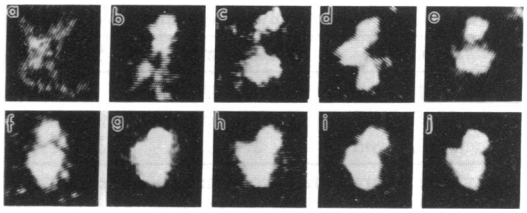

FIG. 5. Gallery of low-pass (30 Å)-filtered electron micrographs illustrating the gradual formation and folding of the three domains of 16S rRNA occurring during the *in vitro* assembly process of the *E. coli* 30S ribosomal subunit. The free 16S rRNA (*a*) attains a medusa-like structure after its interaction with the primary binding proteins (*b*). The subsequent stages of assembly (*c–g*) involve the independent formation of distinct intermediate core particles (complexes III, V, VIII, X, and XII). The fine characteristic features of the native 30S subunit (*j*) are clearly resolved only in the presence of a full complement of proteins (complexes XIII and XIV; *h* and *i*, respectively).

protein addition and protein omission experiments revealed that the association of S3 and S2 depends on prior binding of S14 and S10 (7, 43). Protein–protein crosslinks (20) observed in the 30S subunit between S3–S10 and S3–S4 suggest that S3 may bridge the 3′ and 5′ domains. Since S2 and S3 enhance mutual assembly (7) and crosslinks exist between S2–S8, S2–S5, and S3–S2 (20), it appears that the interactions of S3 are stabilized by its association with S2. Thus, the merging of the head and body involves the interactions of S3 with S10 and S4, and of S2 with S8, S5, and S3. The 30S particles assembled in the absence of protein S5 are deficient in protein S2 and partially deficient in protein S3 (7, 43). Thus, proteins S3 and S2 may be filling up the regions between S10 and S4 and S5 and S8, respectively, leading to the formation of the compact 30S particle.

Incorporation of S21 (Table 1, Complex XIII) enhanced the fine structure of the platform (Fig. 4*g*). S21 is located between proteins S2 and S11, with S11 being at the periphery of the subunit. Although the localization of S21 in the 30S subunit is generally agreed upon (22, 41), there has been some disagreement about its exact binding site on the 16S rRNA. RNA–protein crosslinking studies have shown that S21 crosslinks both to the flexible 3′ end as well as to nucleotide 723 of the central domain (24). S21 binding protects a unique G800 (36), placing the primary site of S21 interaction to the central domain. This interaction results in the full development of the platform by bringing the central and 3′ domains together. Protein–protein crosslinks between S18–S21, S11–S21, S6–S18–S21, and S11–S18–S21 (20) also suggest the proximity of the central domain to the 3′ terminus in the platform structure (24). Finally, the observation that P site-bound tRNA protects bases in the nucleotide 1400, 790, and 690 regions (48) yields further evidence that these regions are indeed very close to one another in the native 30S subunit. The increase in the R_G value (Table 1) could be ascribed to the increase in particle asymmetry after S21 binding.

Attempts to add S1, the last of the proteins involved in the assembly of the *E. coli* subunit, to the reconstituted particles during the assembly process resulted in very poor binding. Since S1 has no significant effect on poly(U)-dependent phenylalanine tRNA binding (7, 43), no attempts were made to enhance reconstitution of the core particles with this protein.

Reconstitution studies were also carried out with total protein (TP30) extracts, which had not been subjected to purification procedures (Table 1, Complex XIV). The protein content of the core particles assayed by SDS/PAGE indicated that most of the proteins bind to the 16S rRNA at a level comparable to that found in the native 30S subunit (Fig. 3). The yield of fully reconstituted particles in both cases was between 30% and 40%. A comparison of the images of reconstituted particles from complex XIII (Fig. 4*g*) and complex XIV (Fig.

Table 2. Poly(U)-dependent polyphenylalanine synthesis

Complex	pmol/pmol*	%†
XIII	3.6–3.9	68
XIV	3.3–3.9	64
30S *E. coli*	5.4–5.5	100

*Range of values representing polyphenylalanine production obtained from several reconstitution experiments.

†The average pmol/pmol value for native 30S subunits was calculated and normalized to 100%. The average value was then calculated for each complex and is shown as a percentage of the 30S control.

4h) along with the native 30S subunit (Fig. *5j*) showed that the fully reconstituted particles, as judged by their morphology and mass values, appear visually similar to the native 30S subunits. Analysis of the polyphenylalanine assays indicates that both complex XIII and complex XIV synthesized between 3.3 and 3.9 pmol of polyphenylalanine per pmol of ribosome, ≈65% of the production observed with the native 30S subunits (Table 2). The R_G values (Table 1) suggest that the reduction in activity could be related to the lower degree of compactness observed for the reconstituted particles.

In summary, visualization of the assembly steps of the 30S subunit from 16S rRNA and its 21 ribosomal proteins demonstrates that the 16S rRNA undergoes significant structural reorganization during this process (Fig. 5). The most striking observation is the formation of intermediate core particles possessing up to three distinct mass centers, which correspond to the 5′, central, and 3′ domains of the 16S rRNA. These domains are brought together in the final stages of assembly by late-binding proteins mostly through protein–protein interactions. This study reports high-resolution imaging of the complete *in vitro* assembly of a cellular organelle from its components and unequivocally establishes that the full complement of small subunit proteins is essential for the precise folding of the 16S rRNA into the characteristic shape of the *E. coli* native 30S ribosomal subunit.

V.M. and S.J.T. contributed equally to this work and should both be considered first authors. We thank W. Hellmann, F. Kito, B. Lin, and Dr. M. N. Simon for excellent technical assistance. J.S.W. and J.F.H. were partially supported by National Institutes of Health Grant RRO1777 and by the U.S. Department of Energy.

1. Hardesty, B. & Kramer, G., eds. (1986) *Structure, Function, and Genetics of Ribosomes* (Springer, New York).
2. Gualerzi, C. O. & Pon, C. L. (1990) *Biochemistry* **29**, 5881–5889.
3. Nierhaus, K. H. (1990) *Biochemistry* **29**, 4997–5008.
4. Hill, W. E., Dahlberg, A., Garrett, R. A., Moore, P. B., Schlessinger, D. & Warner, J. R., eds. (1990) *The Ribosome: Structure, Function and Evolution* (Am. Soc. Microbiol., Washington).
5. Oakes, M., Henderson, E., Scheinman, A., Clark, M. & Lake, J. A. (1986) in *Structure, Function, and Genetics of Ribosomes*, eds. Hardesty, B. & Kramer, G. (Springer, New York), pp. 47–67.
6. Boublik, M., Oostergetel, G. T., Wall, J. S., Hainfeld, J. F., Radermacher, M., Wagenknecht, T., Verschoor, A. & Frank, J. (1986) in *Structure, Function, and Genetics of Ribosomes*, eds. Hardesty, B. & Kramer, G. (Springer, New York), pp. 68–86.
7. Held, W. A., Ballou, B., Mizushima, S. & Nomura, M. (1974) *J. Biol. Chem.* **249**, 3103–3111.
8. Mizushima, S. & Nomura, M. (1970) *Nature (London)* **226**, 1214–1218.
9. Nomura, M. & Held, W. A. (1974) in *Ribosomes*, eds. Nomura, M., Tissières, A. & Lengyel, P. (Cold Spring Harbor Lab., Cold Spring Harbor, NY), pp. 193–223.
10. Dahlberg, A. E. (1989) *Cell* **57**, 525–529.
11. Cundliffe, E. (1990) in *The Ribosome: Structure, Function and Evolution*, eds. Hill, W. E., Dahlberg, A., Garrett, R. A., Moore, P. B., Schlessinger, D. & Warner, J. R. (Am. Soc. Microbiol., Washington), pp. 479–490.
12. Ehresmann, C., Ehresmann, B., Millon, R., Ebel, J.-P., Nurse, K. & Ofengand, J. (1984) *Biochemistry* **23**, 429–437.
13. Ehresmann, C. & Ofengand, J. (1984) *Biochemistry* **23**, 438–445.
14. Moazed, D. & Noller, H. F. (1987) *Nature (London)* **327**, 389–394.
15. Boublik, M., Oostergetel, G. T., Mandiyan, V., Hainfeld, J. F. & Wall, J. S. (1988) *Methods Enzymol.* **164**, 49–63.
16. Mandiyan, V., Tumminia, S., Wall, J. S., Hainfeld, J. F. & Boublik, M. (1989) *J. Mol. Biol.* **210**, 323–336.
17. Tumminia, S. J., Mandiyan, V., Wall, J. S. & Boublik, M. (1991) *Biochimie*, in press.
18. Zimmerman, R. A. (1979) *Methods Enzymol.* **59**, 551–583.
19. Kervalage, A. R., Hasan, T. & Cooperman, B. S. (1983) *J. Biol. Chem.* **258**, 6313–6318.
20. Lambert, J. M., Boileau, G., Cover, J. A. & Traut, R. R. (1983) *Biochemistry* **22**, 3913–3920.
21. Krzyzosiak, W., Denman, R., Nurse, K., Hellmann, W., Boublik, M., Gehrke, C. W., Agris, P. F. & Ofengand, J. (1987) *Biochemistry* **26**, 2353–2364.
22. Capel, M. S., Kjeldgaard, M., Engelman, D. M. & Moore, P. B. (1988) *J. Mol. Biol.* **200**, 65–87.
23. Huang, K. H., Fairdough, R. H. & Cantor, C. R. (1975) *J. Mol. Biol.* **97**, 443–470.
24. Brimacombe, R., Admadja, J., Stiege, W. & Schüler, D. (1988) *J. Mol. Biol.* **199**, 115–136.
25. Schwarzbauer, J. & Craven, G. R. (1985) *Nucleic Acids Res.* **13**, 6767–6786.
26. Powers, T., Stern, S., Changchien, L.-M. & Noller, H. F. (1988) *J. Mol. Biol.* **201**, 697–716.
27. Powers, T., Changchien, L.-M., Craven, G. R. & Noller, H. F. (1988) *J. Mol. Biol.* **200**, 309–319.
28. Nomura, M., Traub, P., Guthrie, C. & Nashimoto, M. (1969) *J. Cell. Physiol.* **74**, 241–251.
29. Nowotny, V. & Nierhaus, K. H. (1988) *Biochemistry* **27**, 7051–7055.
30. Gregory, R. J., Zeller, M. L., Turlow, D. L., Gourse, R. L., Stark, M. J. R., Dahlberg, A. E. & Zimmerman, R. A. (1984) *J. Mol. Biol.* **178**, 287–302.
31. Nomura, M., Mizushima, S., Ozaki, M., Traub, P. & Lowry, C. V. (1969) *Cold Spring Harbor Symp. Quant. Biol.* **34**, 49–61.
32. Held, W. A. & Nomura, M. (1975) *J. Biol. Chem.* **250**, 3179–3184.
33. Stern, S., Powers, T., Changchein, L.-M. & Noller, H. F. (1989) *Science* **244**, 783–790.
34. Ebel, J.-P., Ehresmann, B., Ehresmann, C., Mougel, M., Giege, R. & Moras, D. (1986) in *Structure, Function, and Genetics of Ribosomes*, eds. Hardesty, B. & Kramer, G. (Springer, New York), pp. 270–285.
35. Pleij, C. W. A., Rietveld, K. & Bosch, L. (1985) *Nucleic Acids Res.* **13**, 1717–1731.
36. Stern, S., Powers, T., Changchien, L.-M. & Noller, H. F. (1988) *J. Mol. Biol.* **201**, 683–695.
37. Svensson, P., Changchien, L.-M., Craven, G. R. & Noller, H. F. (1988) *J. Mol. Biol.* **200**, 301–308.
38. Stern, S., Weiser, B. & Noller, H. F. (1988) *J. Mol. Biol.* **204**, 447–481.
39. Schüler, D. & Brimacombe, R. (1988) *EMBO J.* **7**, 1509–1513.
40. Brimacombe, R. (1988) *Biochemistry* **27**, 4207–4214.
41. Stöffler, G. & Stöffler-Meilicke, M. (1986) in *Structure, Function, and Genetics of Ribosomes*, eds. Hardesty, B. & Kramer, G. (Springer, New York), pp. 28–45.
42. Malhotra, A., Tan, R. K.-Z. & Harvey, S. C. (1990) *Proc. Natl. Acad. Sci. USA* **87**, 1950–1954.
43. Buck, M. A. & Cooperman, B. S. (1990) *Biochemistry* **29**, 5374–5379.
44. Girshovich, A. S., Bochkareva, E. S. & Ovchinnikov, Y. A. (1981) *J. Mol. Biol.* **151**, 229–243.
45. Langer, J. A. & Lake, J. A. (1986) *J. Mol. Biol.* **187**, 617–621.
46. Gorini, L. (1974) in *Ribosomes*, eds. Nomura, M., Tissières, A. & Lengyel, P. (Cold Spring Harbor Lab., Cold Spring Harbor, NY), pp. 791–803.
47. Weiner, L. & Brimacombe, R. (1987) *Nucleic Acids Res.* **15**, 3653–3670.
48. Moazed, D. & Noller, H. F. (1990) *J. Mol. Biol.* **211**, 135–145.